URSI GASS 2021, Rome, Italy, 28 August - 4 September 2021

Patient imperceptible WPT for wearable/implantable medical devices

Pablo Pérez-Nicoli*, Martin Sivolella, Nicolás Gammarano, and Fernando Silveira
Instituto de Ingeniería Eléctrica, Facultad de Ingeniería, Universidad de la República. Montevideo, Uruguay.

Abstract

This paper studies the wireless power link for a very low power (5 mW) active implantable medical device (AIMD) with a 25x25 mm receiver coil at a long transmission distance (30 cm minimum). A 2-coil and a 3-coil (adding a resonator) links are evaluated, achieving more than 20 times higher power transfer efficiency in the 3-coil case due to the resonator. This lowers the required output power of the transmitter, simplifying its design and alleviating EM exposure and EMI levels. The presented system would allow to recharge miniaturized AIMDs in a way that is imperceptible for the patient (e.g. from behind the mattress or chair backrest) even when they are implanted deep in the body.

1 Introduction

Wireless Power Transfer (WPT) has proven to be a useful technology to power or recharge devices from smartphones to Active Implantable Medical Devices (AIMDs), allowing a simple recharge process. Most commercially available smartphone charging pads require the phone to lie on the top of it, achieving a transfer distance in the millimeter range. In the case of AIMDs, the user have to lay the charger on his/her clothes, achieving a transfer distance in the few centimeters range, and requiring the user to be aware of this process. If the wireless power link adapts to larger transfer distances, e.g., 30 cm, a more comfortable, non-invasive, and even user-imperceptible recharging scheme can be implemented. Additionally, it would allow to recharge implants that are placed deeper inside the body, acting closer to the target organ.

The limits for increasing the transmission distance in inductive powering for AIMDs were addressed in [1]. Basically, the larger the transmission distance, the lower the Power Transfer Efficiency (PTE), requiring larger power in the transmitter (Tx) to fulfill the receiver (Rx) requirements, thus increasing heat dissipation, generating hazardous voltages in the Tx, and rising concerns about safety (from the electromagnetic exposure point of view) and electromagnetic compatibility (EMC) limits. In [1], a proof-of-concept system was built and measured, transferring 5 mW to a 25x25mm Rx with a transfer distance of 30 cm taking into account the Specific Absorption Rate (SAR) limits [2, 3]. However, the PTE achieved in that link was only 0.09 %, thus 5.56 W were required in the Tx to deliver the 5 mW to the load. Although the system presented in [1] could be used to recharge AIMDs in a more comfortable scheme, e.g., while the patient is sleeping by placing a Tx under the mattress, or or sitting at work, by placing the Tx behind the chair backrest, the system can barely tolerate a distance increase or misalignment generated by the user movements due to the very low PTE even in optimum conditions (perfectly aligned).

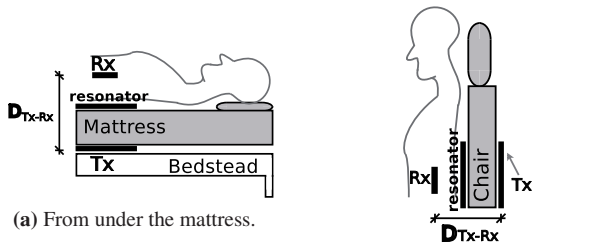

(a) From under the mattress.

(b) From behind chair backrest.

Figure 1. User-imperceptible recharging scheme.

To overcome this PTE degradation at large distances, resonators can be used as in [4, 5]. In this paper, we study the impact of adding a resonator to the 2-coil link proposed in [1]. As a result, we implement a 3-coil proof-of-concept system aimed to power AIMDs that dramatically increases the PTE and improves robustness against user movement compared to [1], as well as allowing power transmission to devices implanted deeply. The proposed system proves the feasibility of a user-imperceptible WPT for wearable and AIMDs in the charging schemes depicted in Fig. 1. The resonator, placed between the Tx and Rx, is a passive element. It can be low-cost, light, and flexible, as it is only composed of a coil (wire loop) and its required resonant capacitor to resonate at the Tx carrier frequency. In the few MHz range, the coil could be a single cable loop connected with some tens of pF capacitor, as in the proof-of-concept system of this work. Such a resonator could be easily embedded in a shirt, above the mattress, or in the chair backrest.
This paper is organized as follows. First, in Section 2, the theoretical analysis is presented, providing expressions useful for the design of the links. Then, in Section 3 the 2-coil link proposed in [1] and the resonator design forming a 3-coil link is presented. Finally, measurement results are reported in Section 4 followed by the conclusion of this work.

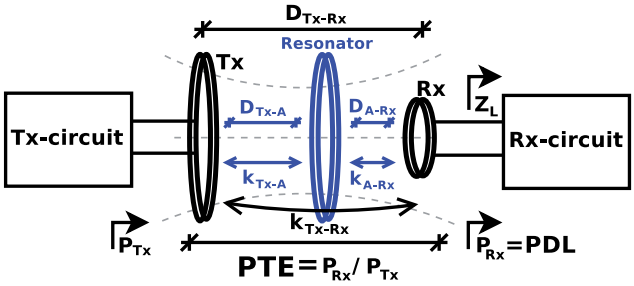

Figure 2. Block diagram of inductive power transmission.

2 Theoretical Analysis

In this section, we present theoretical expressions to calculate the PTE of 2-coil and 3-coil (with resonator) links. Additionally, it is shown in which situations adding a resonator between the Tx and the Rx increases the PTE, in order to predict if a resonator can improve the PTE of the 2-coil link proposed in [1]. In Fig. 2 a simplified block diagram of 2-coil (in black) and 3-coil (adding the blue coil) is presented. The PTE of 2-coil and 3-coil has been widely addressed in previous papers [6, 7]. It is a well-known result that in both cases the PTE depends on the Rx coil load impedance, Z_L in Fig. 2, and an optimum value exists, $Z_{L_{opt}}$, which maximizes the PTE. The imaginary part of $Z_{L_{opt}}$, $\Im(Z_{L_{opt}})$, is the one that achieves the Rx resonance by canceling the Rx coil self inductance. The real part of $Z_{L_{opt}}$ is

$$\begin{aligned}
&\Re(Z_{L_{opt}})_{2\text{-}coil} = R_{Rx}\sqrt{{k_{Tx\text{-}Rx}}^2 Q_{Tx} Q_{Rx} + 1} \\
&\Re(Z_{L_{opt}})_{3\text{-}coil} = \\
&R_{Rx}\sqrt{\frac{{k_{Tx\text{-}A}}^2 Q_{Tx} Q_A + 1}{({k_{A\text{-}Rx}}^2 Q_A Q_{Rx} + 1)({k_{Tx\text{-}A}}^2 Q_{Tx} Q_A + {k_{A\text{-}Rx}}^2 Q_A Q_{Rx} + 1)}},
\end{aligned} \tag{1}$$

where Q_{Tx}, Q_A, and Q_{Rx} are the Tx, resonator, and Rx coils quality factors respectively; $k_{Tx\text{-}A}$, $k_{A\text{-}Rx}$, and $k_{Tx\text{-}Rx}$ are the coupling coefficients between coils as indicated in Fig. 2; and R_{Rx} is the Rx coil Equivalent Series Resistance (ESR).

The $Z_{L_{opt}}$ can be achieved using a matching network, or with more complex circuits as addressed in [8]. Assuming $Z_{L_{opt}}$ is achieved, the PTE of the 2- and 3-coil links are,

$$\begin{aligned}
&\text{PTE} = \frac{A^2 - 1}{(A+1)^2} \qquad \text{where,} \\
&A_{2\text{-}coil} = \sqrt{\underbrace{{k_{Tx\text{-}Rx}}^2 Q_{Tx} Q_{Rx}}_{a_{2\text{-}coil}} + 1} \\
&A_{3\text{-}coil} = \sqrt{\underbrace{\frac{{k_{Tx\text{-}A}}^2 Q_{Tx} Q_A {k_{A\text{-}Rx}}^2 Q_A Q_{Rx}}{{k_{Tx\text{-}A}}^2 Q_{Tx} Q_A + {k_{A\text{-}Rx}}^2 Q_A Q_{Rx} + 1}}_{a_{3\text{-}coil}} + 1}.
\end{aligned} \tag{2}$$

As the PTE is a monotonically increasing function of A, the 3-coil link will have a PTE higher than the 2-coil case if and only if $A_{3\text{-}coil} > A_{2\text{-}coil}$, which is equivalent to

$$\overbrace{\frac{{k_{Tx\text{-}A}}^2 Q_{Tx} Q_A {k_{A\text{-}Rx}}^2 Q_A Q_{Rx}}{{k_{Tx\text{-}A}}^2 Q_{Tx} Q_A + {k_{A\text{-}Rx}}^2 Q_A Q_{Rx} + 1}}^{a_{3\text{-}coil}} > \overbrace{{k_{Tx\text{-}Rx}}^2 Q_{Tx} Q_{Rx}}^{a_{2\text{-}coil}} \tag{3}$$

This result is used in the next section to compare the 2-coil link proposed in [1] and the proposed 3-coil link.

3 Link Design

In this section, we first summarize the Rx description in Section 3.1 which mimics the wireless power Rx of an AIMD. Then, in Section 3.2, we present the design of the 2-coil link proposed in [1] as a benchmark. Finally, in Section 3.3 the proposed 3-coil link is addressed. Both links (2- and 3- coil) are aimed to deliver the required power by the Rx at a transfer distance, $D_{\text{Tx-Rx}}$, of 30 cm which is required by the proposed charging schemes (from under the mattress or behind the chair backrest).

3.1 Rx description and first design decisions

In this paper, we assume that the AIMD requires an average power of 1 mW which is in the order of what is required for various devices such as hearing aid, analog cochlear processor, and body-area monitoring [9]. Assuming that in the proposed user-imperceptible charging scheme depicted in Fig. 1 the AIMD will receive power for at least 5 hours per day, around 5 mW should be delivered to the AIMD while the WPT link is active, to provide enough energy for the daily consumption of 24 mW.h.

The carrier frequency was selected at 13.56 MHz. This frequency is in the Industrial, Scientific and Medical (ISM) band, therefore, the electromagnetic emissions at the carrier frequency are not limited from the EMC point of view. Additionally, this frequency allows the implementation of light and small coils as required by implantable medical devices. For the Rx coil we used the commercial coil model 7001 from Pulse/Larsen, which is a flexible 5 turns 25x25 mm coil satisfying the expected size restrictions imposed by the target application. A picture of this coil is presented in Fig. 3, with the rest of the system, and its self inductance and quality factor are reported in Table 1.

As shown in Fig. 3, the Rx coil is followed by a parallel resonant capacitor and a rectifier loaded by a resistor $R_L = 5.6$ kΩ which models the load, consuming 5 mW at $V_L = 5.3$ V. This desired output voltage is regulated in this work by adjusting the voltage applied to the Tx coil, which is known as a pre regulation scheme. In this case, we used a parallel resonant capacitor, instead of using a series resonant capacitor or a more complex matching network because it is enough to achieve a Z_L very close to the optimum values calculated in (1). The Z_L can be approximated neglecting losses in the rectifier as in [10],

$$Z_L = \Re(Z_L) + j\Im(Z_L) \simeq \frac{2}{R_L(\omega C_{Rx})^2} + \frac{1}{j\omega C_{Rx}}. \tag{4}$$

Selecting $C_{Rx} = 1/(\omega^2 L_{Rx})$, the imaginary part cancels the Rx self inductance, thus $\Im(Z_L) = -j\omega L_{Rx} = \Im(Z_{L_{opt}})$, and the real part is $\Re(Z_L) \simeq 2\ \Omega$ which is very close to both $\Re(Z_{L_{opt}})_{2\text{-}coil}$ and $\Re(Z_{L_{opt}})_{3\text{-}coil}$ as is proven next.

3.2 2-coil link

Since the Rx is assumed to be given, as described in Section 3.1, it only remains the Tx coil design. In this section, we summarize the design presented in [1] as a benchmark to compare it against the proposed 3-coil link presented next.

In [1], it is proven that having a Tx coil radius equal to the target distance maximizes the coupling factor and thus the link efficiency. Therefore the Tx radius was set at 30 cm. Regarding the number of turns, it was proven that if the Tx has more than one turn, the self resonance frequency decreases below the selected carrier frequency. Therefore, the Tx coil is implemented as a single loop, as shown in Fig. 3. The Tx coil self inductance, quality factor, and coupling coefficient to the Rx at the target distance ($D_{\text{Tx-Rx}} = 30$ cm) are reported in Table 1.

Evaluating $\Re(Z_{L_{opt}})_{2\text{-}coil}$ (1) with the values of the parameters reported in Table 1, we obtain $\Re(Z_{L_{opt}})_{2\text{-}coil} = 2.2\ \Omega$, which is close to the approximated value $\Re(Z_L) \simeq 2\ \Omega$, proving that the system is working very close to the optimum load. Then, evaluating $\text{PTE}_{2\text{-}coil}$ (2), we obtain $\text{PTE}_{2\text{-}coil} = 0.09$ % which agrees with the measured value reported in [1]. Finally, evaluating $a_{2\text{-}coil}$ from (3) we obtain $a_{2\text{-}coil} = 0.0037$ which determines the minimum required $a_{3\text{-}coil}$ (3) to improve the PTE.

3.3 3-coil link

In this section, we address the design of a resonator to be placed between the Rx and the Tx described in Sections 3.1 and 3.2 respectively. Based on the theoretical analysis presented in Section 2, the resonator design should maximize $a_{3\text{-}coil}$, as the PTE is a monotonically increasing function of this parameter. Additionally, in the previous section, we found that $a_{3\text{-}coil}$ should be greater than $a_{2\text{-}coil} = 0.0037$, otherwise the resonator will degrade the PTE instead of improving it. To maximize $a_{3\text{-}coil}$, the resonator quality factor, Q_A, and coupling coefficients $k_{T\text{x-}A}$ and $k_{A\text{-}R\text{x}}$ should be as large as possible.

In the proposed charging scheme, the resonator could be placed close to the patient embedded in the chair, clothes or bed linen. In that scheme, there is around 25 cm foam gap between the Tx and the resonator. The distance between the resonator and the Rx could variate from 5 cm or less to 30 cm, depending on the user position, his/her anatomy, and the depth of the implant to be powered. Therefore, the resonator radius was set equal to the Tx radius, 30 cm, maximizing $k_{T\text{x-}A}$ while providing good tolerance to misalignment with the Rx. It must have only one turn, to keep the self resonance frequency higher than the carrier frequency as in the Tx coil design. The self inductance, quality factor, and coupling coefficients at $D_{\text{Tx-A}} = 25$ cm and $D_{\text{A-Rx}} = 5$ cm are reported in Table 1.

Evaluating $\Re(Z_{L_{opt}})_{3\text{-}coil}$ (1) with the values of the parameters reported in Table 1, we obtain $\Re(Z_{L_{opt}})_{3\text{-}coil} = 2\ \Omega$, proving that the system, which has a $\Re(Z_L) \simeq 2\ \Omega$, is still working very close to the optimum load as it was in the 2-coil case. If it had not been the case, it would have been required a modification in the Rx, e.g., a matching network, to match the load. Evaluating $a_{3\text{-}coil}$ from (3) we obtain $a_{3\text{-}coil} = 0.1076$. Therefore, $a_{3\text{-}coil}$ is around 30 times greater than $a_{2\text{-}coil}$ fulfilling (3) and guaranteeing a PTE improvement thanks to the resonator, even under expected variations in distance from Tx to the resonator due to the application. Finally, evaluating $\text{PTE}_{3\text{-}coil}$ (2), we obtain $\text{PTE}_{3\text{-}coil} = 2.5$ %. These results are validated through measurements in the next section.

4 Measurement Results

The measurement setup for the previously described 3-coil link is shown in Fig. 3. To mimic an actual charging scheme, the Tx and resonator are separated by 25 cm foam, and a 5 cm beef separates the resonator and the Rx. The Tx power, $P_{T\text{x}}$, was measured using a shunt resistor of 10 Ω and an oscilloscope. The load voltage, V_L, was measured using a multimeter to calculate P_L as ${V_L}^2/R_L$. The measured efficiency was 2.4 %, validating the previous analysis.

In order to verify the system safety, a SAR simulation was performed as the average over 1 g of tissue using Sim4Life, as shown in Fig. 4, while the link is working as previously described, delivering 5 mW to the load. The maximum value of SAR was 120 mW/kg which is far below the more restrictive (general public) limit of 1.6 W/kg [2, 3].

Finally, keeping the distance between the Tx and the resonator at $D_{\text{Tx-A}} = 25$ cm, we increased the distance between the resonator and the Rx, obtaining $\text{PTE}_{3\text{-}coil} = 2.0$ % at $D_{\text{A-Rx}} = 10$ cm (thus $D_{\text{Tx-Rx}} = 35$ cm) and $\text{PTE}_{3\text{-}coil} = 0.29$ % at $D_{\text{A-Rx}} = 30$ cm (thus $D_{\text{Tx-Rx}} = 55$ cm), showing the system robustness compared to the 2-coil link which has only 0.09 % at $D_{\text{Tx-Rx}} = 30$ cm.

5 Conclusion

The design and measurement of a 3-coil link for WPT at long distance (30 cm minimum) has shown that the PTE can be increased more than 20 times compared to a 2-coil design. This is achieved while placing the third, resonator, coil at 25 cm from the Tx coil and 5 cm from the Rx coil. This position is compatible with an AIMD implanted at a standard depth and power transfer from behind the mattress or chair backrest, while the 3rd coil could be embedded in the patient cloths, bed linen or front of the chair backrest. Furthermore, if the Rx coil is separated 30 cm from the resonator (a case that could approximately mimic a change in position of the patient or the case of a deeply implanted AIMD), still the desired power transfer is achieved with approximately 3 times better PTE than when only 2 coils are used. The increase in power transfer efficiency simplifies the Tx design and improves EM exposure, which is shown to be largely below the established limits.

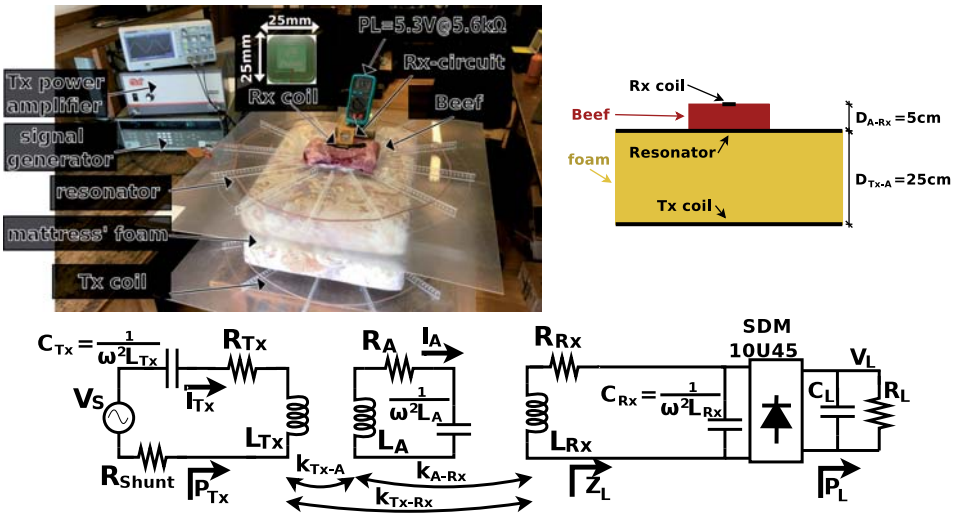

Figure 3. Measurement setup and circuit schematic. The R_{Tx}, R_A, and R_{Rx} model the ESR of the Tx coil, resonator, and Rx coil respectively. The $R_{shunt} = 10\ \Omega$ was included to measure the Tx current. Parameters' values are presented in Table 1.

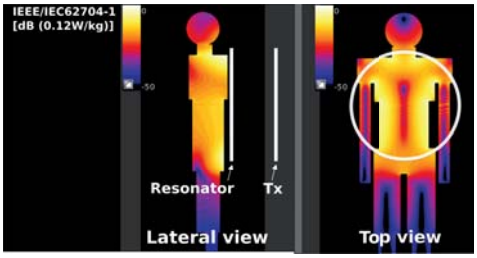

Figure 4. SAR simulation using Sim4Life.

Table 1. Parameters of the practical example.

Parameters		Value
Tx coil	L_{Tx}	2.2 μH
Diameter, ⌀ 60 cm	Q_{Tx}	71
Resonator	L_A	2.2 μH
Diameter, ⌀ 60 cm	Q_A	200
Rx coil	L_{Rx}	877 nH
□ 25 × 25 mm	Q_{Rx}	34
$D_{\text{Tx-A}}$; $k_{Tx\text{-}A}$		25 cm ; 0.1
$D_{\text{A-Rx}}$; $k_{A\text{-}Rx}$		5 cm ; 0.004
$D_{\text{Tx-Rx}}$; $k_{Tx\text{-}Rx}$		30 cm ; 0.0012
Carrier frequency, f_S		13.56 MHz
Load power P_L (V_L @ R_L)		5 mW (5.3 V@5.6 $k\Omega$)
$a_{2\text{-}coil}$ evaluating (3)		0.0037
$a_{3\text{-}coil}$ evaluating (3)		0.1076
$\text{PTE}_{(2\text{-}coil)}$ evaluating (2)		0.09 %
$\text{PTE}_{(3\text{-}coil)}$ evaluating (2)		2.5 %
$\text{PTE}_{(2\text{-}coil)} = P_L/P_{Tx}$, measured		0.09 %
$\text{PTE}_{(3\text{-}coil)} = P_L/P_{Tx}$, measured		2.4 %

6 Acknowledgements

We thank Sim4Life by ZMT for providing the simulation software, CSIC Universidad de la República and ANII FMV 1 2017 1 136740 for the financial support.

References

[1] P. Pérez-Nicoli, *et al.*, "Limits for increasing the WPT distance in AIMDs," in *33st URSI Gen. Assem. Sci. Symp.* IEEE, 2020, pp. 1–4.

[2] H. M. Madjar, "Human radio frequency exposure limits: An update of reference levels in Europe, USA, Canada, China, Japan and Korea," in *IEEE Int. Symp. Electromagn. Compat.* IEEE, 2016, pp. 467–473.

[3] A. Christ, *et al.*, "Assessing human exposure to electromagnetic fields from wireless power transmission systems," *Proc. IEEE*, vol. 101, no. 6, pp. 1482–1493, 2013.

[4] A. Kurs, *et al.*, "Wireless power transfer via strongly coupled magnetic resonances," *Science*, vol. 317, no. 5834, pp. 83–6, July 2007.

[5] T. Sun, *et al.*, "A two-hop wireless power transfer system with an efficiency-enhanced power receiver for motion-free capsule endoscopy inspection," *IEEE Trans. Biomed. Eng.*, vol. 59, no. 11, pp. 3247–3254, Nov. 2012.

[6] M. Kiani and M. Ghovanloo, "The circuit theory behind coupled-mode magnetic resonance-based wireless power transmission," *IEEE Trans. Circuits Syst. I*, vol. 59, no. 9, pp. 2065–2074, Sep. 2012.

[7] P. Pérez-Nicoli and F. Silveira, "Matching networks for maximum efficiency in two and three coil wireless power transfer systems," in *IEEE Latin Amer. Symp. Circuits Syst.* IEEE, Feb. 2016, pp. 215–218.

[8] P. Pérez-Nicoli and F. Silveira, "Maximum efficiency tracking in inductive power transmission using both matching networks and adjustable AC-DC converters," *IEEE Trans. Microw. Theory Techn.*, vol. 66, no. 7, pp. 3452–3462, 2018.

[9] A. P. Chandrakasan, *et al.*, "Ultralow-power electronics for biomedical applications," *Annu. Rev. Biomed. Eng.*, vol. 10, pp. 247–274, 2008.

[10] P. Pérez-Nicoli and F. Silveira, "Maximum efficiency point tracking in inductive links: Series versus parallel receiver's compensation," in *IEEE Wireless Power Transf. Conf.* IEEE, 2019, pp. 150–153.